ORIGINAL ARTICLE

Developing an Analytical Model for Knife-Edge Slit Collimator Optimization for Prompt Gamma Imaging in Proton Therapy

Etesam Malekzadeh *

Department of Medical Physics, Faculty of Medical Sciences, Tarbiat Modares University, Tehran, Iran

*Corresponding Author: Etesam Malekzadeh
Email: e.malekzadeh@modares.ac.ir

Received: 15 August 2022/ Accepted: 18 September 2022

Abstract

Purpose: Gamma cameras are one of the most promising technologies for in-vivo range monitoring in proton therapy. Monte Carlo (MC) simulation is a common calculation-based technique to design and optimize gamma cameras. However, it is prohibitively time-consuming. Analytical modeling speeds up the process of finding the optimal design.

Materials and Methods: We proposed an analytical method using the efficiency-resolution trade-off for optimizing a knife-edge collimator based on the range retrieval precision of protons. Monte Carlo simulation was used for validation of obtained collimator efficiencies.

Results: The model predicts that for the optimal range retrieval precision, the ratio of the source-to-detector distance (r_d) to the source-to-collimator distance (r_c) should be ranging from 1.7 to 1.9. For a special case, it was found that assuming an ideal detector ($R_i = 0$), the falloff retrieval precision is optimal at $r_d = 2r_c$ independent of the collimator resolution. Moreover, using the optimized camera, the difference between the MC calculated range and the absolute range was 0.5 cm (the relative error is about 3%).

Conclusion: It was found that the collimator parameters are in good agreement in comparison with that of the MC results reported in the literature. The analytical method studied in this work can be used to design and optimize imaging systems based on KE collimators in combination with new detectors in a fast and reliable way.

Keywords: Monte Carlo; Gamma Camera; Range Verification; Proton Therapy; Analytical Optimization.

DOI: https://doi.org/10.18502/fbt.v10i4.13725

1. Introduction

Proton Therapy (PT) has several advantages over x-ray radiation therapy including maximum dose deposition at a certain depth inside the so-called Bragg peak and rapid dose fall-off beyond it [1, 2]. These characteristics offer a highly tailored radiation dose to the tumor volume with good sparing of normal tissues as well as eliminating the exit dose. However, the finite range of proton beams mandates accurate proton range estimation in a patient body that is a big challenge and associates with range uncertainties [3]. Range uncertainties have several sources such as patient positioning, movement of the patients, internal organ motions, artifacts in the Computed Tomography (CT) images, and uncertainty in treatment planning are the sources of error in proton range estimation [2]. Thus, to exploit the potential of proton therapy, it is necessary to minimize the treatment uncertainties [4].

Several solutions have been proposed to address the range verification in proton therapy to assess the compliance between the delivered and prescribed dose [5-7]. Instruments based on Prompt-Gamma (PG) detection have been investigated using Monte Carlo (MC) simulation for range verification in PT [8-10]. PG rays are promptly emitted after beam interactions with matter and have a wide energy spectrum ranging from 1 to 8 MeV [11]. Among the proposed cameras, the Knife-Edge (KE) camera has been designed, tested, and used in clinics. The KE collimator is a modified type of pinhole collimator with a long channel in the longitudinal direction that increases the camera efficiency [12]. In the PG-imaging context, Smeets *et al.* [12], in their comprehensive study, optimized the KE camera considering the 1:1 (image size: object size) image projection. However, they ignored the image magnification factor, which is defined as the focal length to the source-to-collimator ratio. In another study, Bom *et al.* optimized the KE camera for range verification in double-scattered proton beam cases [13]. They have taken into account the magnification factor to improve the camera resolution. However, MC is a time-consuming tool to assess all of the possible magnification factors for optimizing the camera.

Slit collimators have been investigated using MC simulations for molecular imaging and particle therapy applications. Mahani *et al.* conducted an MC optimization study of a new type of rotating slit collimator for small animal imaging [14]. Lopes *et al.* proposed an analytical formula for the KE collimator and investigated the detection efficiency and resolution trade-off in collimator optimization [15]. However, it has been demonstrated that their derived formula has some deviations from the proposed formula for the slit collimator and the MC results [16, 17]. In another study, a comprehensive MC-based simulation was reported for the KE and MPS collimators. These results include the penetration and scattering effect. However, the used MC GEANT4 code is time-consuming for checking all of the possible configurations of the collimator parameters [18]. In another research, the slit collimator was studied experimentally by Priegnitz *et al.* who presented slit camera measurements of prompt gamma depth profiles in inhomogeneous targets [19]. According to their study, different range verification scenarios require special resolution and sensitivity of the slit collimator. Therefore, an analytical model is highly needed for adjusting the collimator parameters to obtain desired results.

Unlike MC, analytical methods make a quick assessment of various imaging parameters. Therefore, a collimator design and optimization are possible with analytical methods [20]. To the best of our knowledge, no analytical model has been reported for the KE collimator resolution and efficiency optimization purposes. This study aims (i) to develop an optimization method based on the Fall-off Retrieval Precision (FRP) concept [1, 21] that defines a relationship between the efficiency and the detected range, introduced by Roellinghoff *et al.* for multi-parallel slat collimator [21] and (ii) to find out that there is an optimum design configuration independent of any added corrections for a given fixed resolution and a source-to-collimator distance. Consequently, the model was simplified by ignoring the photons' penetration /scattering through the collimator wall to fully concentrate on the geometric trade-off between the resolution and geometric efficiency.

2. Materials and Methods

2.1. Collimator Setup

The schematic diagram of a KE camera used for the analytical system model is shown in Figure 1 and its geometric parameters are listed in Table 1. We used the simulation setup introduced by Smeets *et al.* [12]. According to Figure 1, the z-axis (perpendicular to the plane) lies along the centerline of the slit, and the KE

channel, as well as detector length along the z-axis, are L and w', respectively. In this study, the detector length (L = 200 mm) was chosen as a fixed parameter considering the available crystal length (Figure 2). Collimator optimization was done considering the single 4.4 MeV isotropic point source. The 4.4 MeV is the Carbon nuclei characteristics energy line and is considered the most significant energy line in the prompt gamma energy spectrum and is used as the mean energy of the spectrum for the optimization studies in the range verification context [22]. The source was positioned at $(x = 0, y = -rc, z = 0)$. Tungsten's linear attenuation coefficient is $\mu = 0.078\ mm^{-1}$ for this energy. The phantom material is PMMA with 15.0 cm and 20.0 cm of diameter and length, respectively. The detector material is LYSO and its length and width are 20.0 cm and 10.0 cm, respectively. The collimator is made of tungsten with a 4.0 cm thickness.

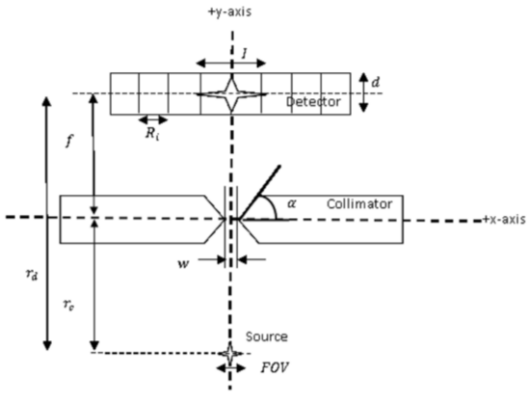

Figure 1. Geometric description of physical parameters of the KE collimator. Magnification factor (M) is defined as image size (I) to a FOV (I/FOV) ratio as illustrated in the figure

Table 1. The summary of the camera parameters.

Description	Parameter	Description	Parameter
Slit opening angle	α	Source to detector distance	r_d
Slit aperture width	w	Source to collimator distance	r_c
Scintillator length	L	Detector intrinsic resolution	R_i
Scintillator thickness	d	Focal length	f
System resolution	R_{sys}	System efficiency	g_{sys}

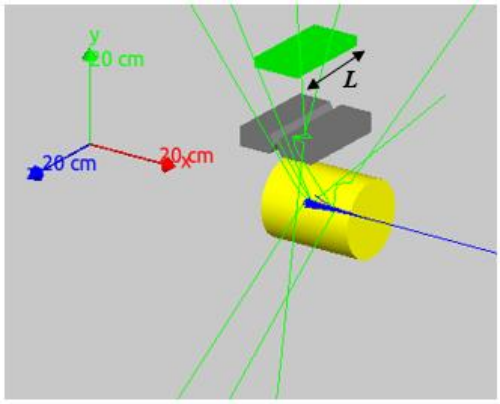

Figure 2. Simulation setup was illustrated using the Qt software in the GATE Monte Carlo package. L is the scintillator length along the z-axis

2.2. Mathematical Model

To determine the imaging system parameters that provide the best performance, our optimization procedure is based on the method described by Rentmeester *et al.* [23]. This method is based on the geometric trade-off between system resolution and efficiency. According to this method, a relationship must be obtained between the resolution and the efficiency of the collimator.

An adaptation of Metzler's method [24] was used to provide a way of calculating the resolution of the camera (R_{sys}). According to this method, it was assumed that the total resolution of the KE collimator can be calculated by combining the KE collimator resolution R_{KE} and intrinsic resolution R_i of the pixelated detector that is given by the following Equation.

$$R_{sys} = \left[R_{KE}^2 + \left(\frac{r_c}{r_d - r_c}\right)^2 R_i^2\right]^{\frac{1}{2}} \quad (1)$$

In Equation 1, R_{KE} is the KE collimator geometrical resolution given with the following Equation:

$$R_{KE} = w\frac{r_d}{r_d - r_c} \quad (2)$$

The collimator efficiency (g_{coll}) of the KE slit camera can be written in the following way [16] (Equation 3):

$$g_{coll} = \frac{wL}{4\pi r_d r_c} \quad (3)$$

By combining Equation 1 and Equation 3, the collimator efficiency g_{coll} was calculated using the following way:

$$g_{coll} = \left[R_{sys}^2 - \left(\frac{r_c}{r_d - r_c}\right)^2 R_i^2\right]^{\frac{1}{2}} \frac{L(r_d - r_c)}{4\pi r_d^2 r_c} \quad (4)$$

The system optimization considering the Bragg peak detection was investigated based on the FRP concept which defines a relationship between a total number of impinging radiation and the precision of the detected range [21]. Fall-off retrieval precision was proposed by Roellinghoff *et al.* for the performance evaluation of the imaging system considering the range calculations [21]. Generally, other researchers mentioned this parameter as range precision calculations that related to the number of incident particles on phantom/patient [10, 12, 25, 26]. The geometric efficiency is defined as the fraction of isotropically emitted photons, $N_{emitted}$, which are appropriately collimated, $N_{detected}$ and can be written as follows [27] (Equation 5):

$$g_{coll} = \frac{N_{detected}}{N_{emitted}} \quad (5)$$

It can be seen for a given number of emitted prompt gamma photons, the geometric efficiency is correlated to the number of detected photons as $g_{coll} \propto N_{detected}$. The formula can be written in the following way (Equation 6):

$$FRP = \frac{1}{\sqrt{g_{coll}}} \quad (6)$$

Therefore, from the optimization point of view, one can consider FRP as $FRP = \frac{1}{\sqrt{g_{coll}}}$. Here, FRP acts as a relativistic metric to compare the designs and select the best one. Here, we used an adaption of the formula with some modifications according to the above-mentioned justification. It is obvious that higher geometric sensitivities lead to passing more photons from the collimator. Accordingly, more detected photons lead to an increase in contrast (i.e., count difference before and after Bragg peak), which directly is related to Bragg peak fall-off retrieval [12]. Therefore, the higher the geometric sensitivity is, the better the FRP achieves.

We developed a code in C++ program, which enabled us to find the geometrical parameters of the detector and collimator that provide the best system efficiency and resolution. Using the code, the FRP was investigated with a fixed system resolution at R_{sys}= 12.0, 14.0, 16.0, and 18.0 mm. These values were selected according to the available spatial resolutions for the developed knife-edge camera [12]. The source-to-collimator distance was fixed at r_c = 150.0 mm (the minimum radius allowed in clinical brain imaging that is compatible with proton treatments on head-and-neck district) and the source-to-detector distance (r_d) was varied from a minimum of 165.0 mm to a maximum of 500.0 mm which in turn varied the focal length f from a minimum of 15.0 mm to a maximum of 350.0 mm. The same procedure was repeated for the same fixed system resolution at R_{sys}= 18.0 mm, but this time the source-to-collimator distance r_c was considered fixed at 130.0, 150.0, 170.0, and 190.0 mm.

2.3. Monte Carlo Simulation

MC simulations were performed with GATE/GEANT4 package version 8.2 [28]. This version of GATE is based on the GEANT4 version 10.5.1. GATE is an open-source software based on the GEANT4 toolkit designed for the modeling and design of tomographic imaging systems such as Positron Emission Tomography (PET) and Single-Photon Emission Computed Tomography (SPECT) as well as radiotherapy applications [29]. Therefore, it is a suitable tool for simulation in diagnostic-therapeutic research [30]. For modeling the transport of the particles, the QGSP_BIC_HP_EMY physics list was used for beam interactions with matter [31]. This physics list includes appropriate models of nuclear interactions that are in good agreement with the experimental results obtained for prompt gamma. In proton therapy, energies are used in the range of 60 MeV (for the treatment of ocular tumors) to 240 MeV (for the treatment of deep tumors) [3,32]. In this research, 160 MeV was selected to irradiate the PMMA ($(C_5H_8O_2)_n$, density = 1.19 g/cm^3) phantom. A total number of 10^8 protons were simulated to consider the realistic single-spot pencil beam in treatment [31]. The proton beam was considered a fully ideal pencil beam without any energy, spatial, or angular distributions [12].

3. Results

3.1. System Optimization Considering the FRP

The KE collimator optimization was investigated considering the Bragg peak retrieval along the beam axis and its dependency on the geometrical parameters of the collimator and detector. The dependence of the FRP on the source-to-collimator and source-to-detector distance was studied at fixed system resolution. Figure 3a shows that the FRP of the KE collimator improves with increasing the source-to-detector distance, reaches the

optimum value, and then deteriorates with a further increase in detector distance. This means that there is an optimum FRP at which the KE collimator has the best performance. Moreover, the distance of the source-to-detector at which the FRP reaches its optimum varies with source-to-collimator distance r_c (Figure 3b). For system resolution of R_{sys} = 18.0 mm, this optimal source-to-detector distance is r_d = 245.0, 280.0, 320.0, and 360.0 mm for which the FRP = 28.0, 32.0, 37.0 and 41.0, respectively. For a focal length less than 55.0 mm there is no value for FRP. In Figure 3c, the results of the FRP against $\frac{r_d}{r_c}$ ration for different source-to-collimator distances show that there is a $\frac{r_d}{r_c}$ ratio at which FRP is optimal for the KE collimator and that is found to be in the range of 1.7-1.9.

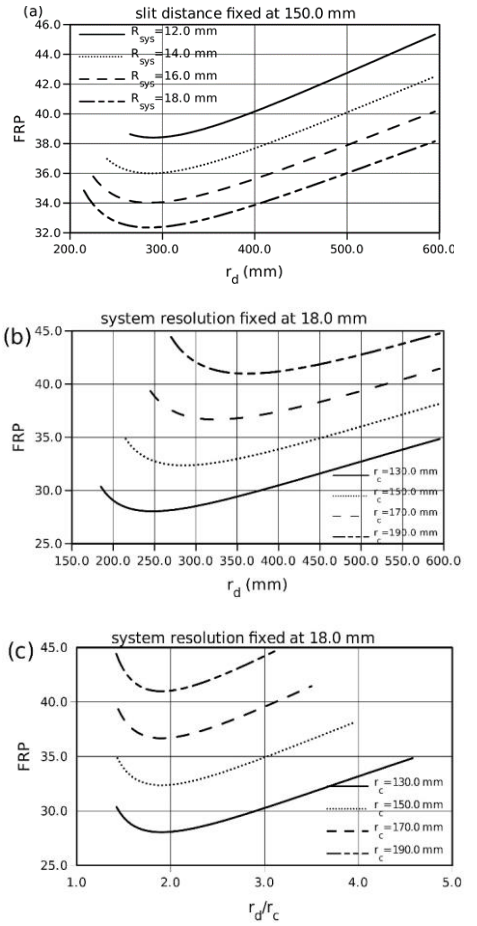

Figure 3. The KE collimator optimization results considering the Bragg peak retrieval for a fixed system resolution R_{sys} at 12.0, 14.0, 16.0, and 18.0 mm (r_c fixed at 130.0 mm). (a) The figures show the resulting system FRP as a function of the detector distance r_d for fixed source-to-collimator distance, and (b) for fixed system resolution R_{sys}= 18.0 mm. In (c) FRP is plotted as a function of the $\frac{r_d}{r_c}$ ratio for different fixed r_c= 130.0, 150.0, 170.0 and 190.0 mm

3.2. FRP and Range Quantification

MC simulation was used for the validation of the optimized system performance. To do so, the 160 MeV proton range in the PMMA phantom was estimated using the optimized KE camera (Figure 2). The range of 160 MeV protons is 15.2 cm in the PMMA phantom. Consequently, as can be seen from Figure 4, the differences between the MC calculated and the absolute ranges were 0.5 cm (the relative error is about 3%). The MC results for the camera efficiency were reported in Table 2. Since the radiation penetration through the collimator slit was ignored in theoretical calculations, the MC predicted

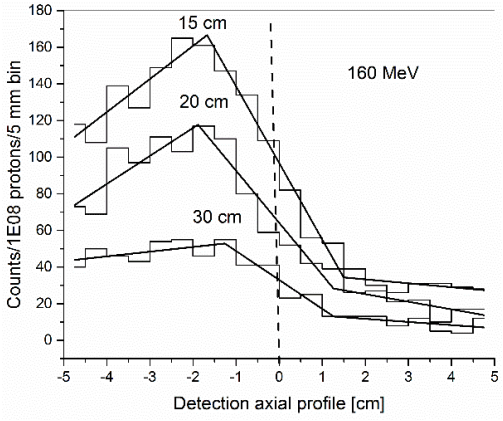

Figure 4. The Detection profile of PGs produced by a 160 MeV proton beam is illustrated for three different source-to-collimator distances

Table 2. Calculated values for the resolution, efficiency, and FRP

Source-to-collimator distance (mm)	Source-to-detector distance (mm)	Resolution (mm)	Slit opening angle (degree)	Slit aperture width (mm)	Efficiency	Efficiency (MC)	FRP
130	260	12	60	6	2.8E-03	5.1E-03	19
150	300	12	63	6	2.1E-03	4.9E-03	22
170	340	12	66	6	1.6E-03	3.4E-03	25
190	380	12	68	6	1.3E-03	3.5E-03	28

results are approximately 2-fold more than that of theory. Additionally, FRP values were calculated theoretically, and the results were reported in Table 2. With taking the derivative of Equation 4, the optimal detector distance value was calculated assuming the ideal detector $R_i = 0$. It was found that for any fixed resolution, the system efficiency is maximum at $r_d = 2r_c$ independent of the resolution.

4. Discussion

In this study, an analytical method was developed and applied for the KE collimator modeling and optimizing for range verification. The concept of FRP was successfully developed and applied for the KE collimator in this research. Moreover, the response of the detector in terms of an intrinsic resolution was considered. It was found that in the context of proton range verification, despite some simplifications such as ignoring the scattered photons and neutron-induced secondary gammas, analytical methods can be implemented for a better understanding of the relationship between collimator parameters and imaging metrics such as spatial resolution and efficiency.

Based on the characteristic curves (Figure 3), which are plotted using derived formulas, we studied the variation of the FRP to optimize the KE collimator. It was found that there is an optimal value for each characteristic curve at the $\frac{r_d}{r_c}$ = 1.8 ratios when detectors are used with R_i = 4.0 mm. For R_i = 0.0 mm, the optimal ratio is $\frac{r_d}{r_c}$ = 2.0, which is slightly different in comparison to that of the R_i = 4.0 mm case (Table 2). Therefore, this ratio varies with the detector response. This result is remarkably important to speed up camera design by considering different detectors [33]. Moreover, in this study, it was found that the source-to-detector distance at which the characteristic curve reaches its optimum varies with the source-to-collimator distance (Figure 3b). It is interesting to note that for a fixed slit distance r_c = 150.0 mm (suitable for the design of the head and neck tumor imaging system), the FRP at the source-to-detector distance of r_d = 290.0 mm is optimal independent of the system resolution (Figure 3a). This result is in good agreement with the optimized KE camera parameters suggested by Smeets *et al.* [12].

The main aim of this study was to develop an analytical slit collimator model and to prove that there is an optimum configuration, which maximizes the geometric efficiency for a given fixed resolution and the source-to-collimator distance. Consequently, we observed the agreement in trends of geometric efficiency and MC results. However, absolute values are far from expected because of the lack of scattering/penetration and also neutron background modeling in this study. Penetration and scattering add a constant amount (up to 2-fold) to the resolution and geometric efficiency, however, it can be seen from the results that different resolution values do not change the optimum detector distance to slit distance ratio (that is 1.7-1.9) (Figure 3). Consequently, it was found that the optimum ratio is distance independent. Finally, penetration/scattering and neutron background modeling are under the study for future developments of the proposed model and are not the aim of this study.

Smeets *et al.* have optimized the KE camera for $r_d = 2r_c$ (magnification factor M = 1) [12]. So, our findings support their results despite ignoring the penetration and scattering effect. In another study, Bom *et al.* [13] suggested that the magnification factors greater than M = 1 are the optimal case in range monitoring. It seems that considering the scattering effect, the magnification factor of more than 1 is a better choice to take into account the KE collimator magnification capability and also decreasing the scattered photons. However, more investigations are needed to assess this postulation using the analytical developed method.

Several studies have previously addressed the single-pinhole/slit-slat collimator modeling generalization to multi-pinhole/multi-slit-slat collimators [23, 34]. Consequently, our derived model may also be applied for multi-slit collimator design as the whole geometric sensitivity of the multi-slit collimator could be considered by multiplying the single-slit collimator's formula. However, further theoretical and simulation studies are required to validate this generalization. Analytical models are efficient methods in proton therapy. The developed model could be useful for designing adaptive slit collimators, which is necessary for range verification in different clinical beam delivery scenarios. Furthermore, as the collimator-based cameras, optimum performance is distance dependent [6], therefore the model may provide advantageous information for fast or maybe online optimizing the adjustable slit collimator in the clinic.

5. Conclusion

The importance of this research lies both in its speed and its relative ease of application to new detector types such as pixelated or monolithic crystals. Also, the developed method can be generalized to other collimator systems such as a parallel hole or cone-beam gamma camera. The developed method allowed a significantly fast reproduction of the KE camera parameters in comparison to the MC simulation with an acceptable difference. However, it is important to consider realistic PG source distributions in this model as well.

Acknowledgments

This research did not receive any specific grant from funding agencies in the public, commercial, or not-for-profit sectors.

References

1- J Krimmer, D Dauvergne, JM Létang, and É Testa, "Prompt-gamma monitoring in hadrontherapy: A review." *Nuclear Instruments and Methods in Physics Research Section A: Accelerators, Spectrometers, Detectors and Associated Equipment*, Vol. 878pp. 58-73, (2018).

2- Harald Paganetti, "Range uncertainties in proton therapy and the role of Monte Carlo simulations." *Physics in Medicine & Biology*, Vol. 57 (No. 11), p. R99, (2012).

3- Marco Durante and Jay S Loeffler, "Charged particles in radiation oncology." *Nature reviews Clinical oncology*, Vol. 7 (No. 1), pp. 37-43, (2010).

4- Sebastian Tattenberg, Thomas M Madden, Bram L Gorissen, Thomas Bortfeld, Katia Parodi, and Joost Verburg, "Proton range uncertainty reduction benefits for skull base tumors in terms of normal tissue complication probability (NTCP) and healthy tissue doses." *Medical physics*, (2021).

5- Marco Toppi *et al.*, "Monitoring carbon ion beams transverse position detecting charged secondary fragments: results from patient treatment performed at CNAO." *Frontiers in oncology*, Vol. 11(2021).

6- Aleksandra Wrońska, "Prompt gamma imaging in proton therapy-status, challenges and developments." in *Journal of Physics: Conference Series*, (2020), Vol. 1561 (No. 1): *IOP Publishing*, p. 012021.

7- Yunhe Xie *et al.*, "Prompt gamma imaging for the identification of regional proton range deviations due to anatomic change in a heterogeneous region." *The British Journal of Radiology*, Vol. 93 (No. 1116), p. 20190619, (2020).

8- Hyun Joon Choi, Ji Won Jang, Wook-Geun Shin, Hyojun Park, Sebastien Incerti, and Chul Hee Min, "Development of integrated prompt gamma imaging and positron emission tomography system for in vivo 3-D dose verification: a Monte Carlo study." *Physics in Medicine & Biology*, Vol. 65 (No. 10), p. 105005, (2020).

9- Elisa Fiorina *et al.*, "Detection of inter-fractional morphological changes in proton therapy: a simulation and in-vivo study with the INSIDE in-beam PET." *Frontiers in Physics*, Vol. 8p. 660, (2020).

10- Wenzhuo Lu *et al.*, "Simulation Study of a 3D Multi-slit Prompt Gamma Imaging System for Proton Therapy Monitoring." *IEEE Transactions on Radiation and Plasma Medical Sciences*, (2021).

11- Marco Durante and Harald Paganetti, "Nuclear physics in particle therapy: a review." *Reports on Progress in Physics*, Vol. 79 (No. 9), p. 096702, (2016).

12- Julien Smeets *et al.*, "Prompt gamma imaging with a slit camera for real-time range control in proton therapy." *Physics in Medicine & Biology*, Vol. 57 (No. 11), p. 3371, (2012).

13- Victor Bom, Leila Joulaeizadeh, and Freek Beekman, "Real-time prompt gamma monitoring in spot-scanning proton therapy using imaging through a knife-edge-shaped slit." *Physics in Medicine & Biology*, Vol. 57 (No. 2), p. 297, (2011).

14- Hojjat Mahani, Gholamreza Raisali, Alireza Kamali-Asl, and Mohammad Reza Ay, "Spinning slithole collimation for high-sensitivity small animal SPECT: Design and assessment using GATE simulation." *Physica Medica*, Vol. 40pp. 42-50, (2017).

15- P Cambraia Lopes *et al.*, "Optimization of collimator designs for real-time proton range verification by measuring prompt gamma rays." in *2012 IEEE Nuclear Science Symposium and Medical Imaging Conference Record (NSS/MIC)*, (2012): *IEEE*, pp. 3864-70.

16- Etesam Malekzadeh, Hossein Rajabi, Elisa Fiorina, and Faraz Kalantari, "Derivation and validation of a sensitivity formula for knife-edge slit gamma camera: A theoretical and Monte Carlo simulation study." *Iranian Journal of Nuclear Medicine*, Vol. 29 (No. 2), pp. 86-92, (2021).

17- Gengsheng L Zeng and Daniel Gagnon, "CdZnTe strip detector SPECT imaging with a slit collimator." *Physics in Medicine & Biology*, Vol. 49 (No. 11), p. 2257, (2004).

18- Jong Hoon Park *et al.*, "Comparison of knife-edge and multi-slit camera for proton beam range verification by Monte Carlo simulation." *Nuclear Engineering and Technology*, Vol. 51 (No. 2), pp. 533-38, (2019).

19- M Priegnitz *et al.*, "Measurement of prompt gamma profiles in inhomogeneous targets with a knife-edge slit

camera during proton irradiation." *Physics in Medicine & Biology*, Vol. 60 (No. 12), p. 4849, (2015).

20- Saree Alnaghy *et al.*, "Analytical modelling and simulation of single and double cone pinholes for real-time in-body tracking of an HDR brachytherapy source." *IEEE Transactions on Nuclear Science*, Vol. 63 (No. 3), pp. 1375-85, (2016).

21- F Roellinghoff *et al.*, "Real-time proton beam range monitoring by means of prompt-gamma detection with a collimated camera." *Physics in Medicine & Biology*, Vol. 59 (No. 5), p. 1327, (2014).

22- Jerimy C Polf *et al.*, "Measurement of characteristic prompt gamma rays emitted from oxygen and carbon in tissue-equivalent samples during proton beam irradiation." *Physics in Medicine & Biology*, Vol. 58 (No. 17), p. 5821, (2013).

23- MCM Rentmeester, F Van Der Have, and FJ Beekman, "Optimizing multi-pinhole SPECT geometries using an analytical model." *Physics in Medicine & Biology*, Vol. 52 (No. 9), p. 2567, (2007).

24- Scott D Metzler, Roberto Accorsi, John R Novak, Ahmet S Ayan, and Ronald J Jaszczak, "On-axis sensitivity and resolution of a slit-slat collimator." *Journal of Nuclear Medicine*, Vol. 47 (No. 11), pp. 1884-90, (2006).

25- John Ready, "Development of a multi-knife-edge slit collimator for prompt gamma ray imaging during proton beam cancer therapy." *UC Berkeley*, (2016).

26- Hsin-Hon Lin, Hao-Ting Chang, Tsi-Chian Chao, and Keh-Shih Chuang, "A comparison of two prompt gamma imaging techniques with collimator-based cameras for range verification in proton therapy." *Radiation Physics and Chemistry*, Vol. 137pp. 144-50, (2017).

27- Stephen C Moore, Kypros Kouris, and Ian Cullum, "Collimator design for single photon emission tomography." *European journal of nuclear medicine*, Vol. 19 (No. 2), pp. 138-50, (1992).

28- Sea Agostinelli *et al.*, "GEANT4—a simulation toolkit." *Nuclear Instruments and Methods in Physics Research Section A: Accelerators, Spectrometers, Detectors and Associated Equipment*, Vol. 506 (No. 3), pp. 250-303, (2003).

29- Karine Assie *et al.*, "Monte Carlo simulation in PET and SPECT instrumentation using GATE." *Nuclear Instruments and Methods in Physics Research Section A: Accelerators, Spectrometers, Detectors and Associated Equipment*, Vol. 527 (No. 1-2), pp. 180-89, (2004).

30- Sébastien Jan *et al.*, "GATE V6: a major enhancement of the GATE simulation platform enabling modelling of CT and radiotherapy." *Physics in Medicine & Biology*, Vol. 56 (No. 4), p. 881, (2011).

31- Estelle Hilaire, David Sarrut, Françoise Peyrin, and Voichiţa Maxim, "Proton therapy monitoring by Compton imaging: influence of the large energy spectrum of the prompt-γ radiation." *Physics in Medicine & Biology*, Vol. 61 (No. 8), p. 3127, (2016).

32- Edward C Halperin, "Particle therapy and treatment of cancer." *The lancet oncology*, Vol. 7 (No. 8), pp. 676-85, (2006).

33- Guntram Pausch *et al.*, "Detection systems for range monitoring in proton therapy: Needs and challenges." *Nuclear Instruments and Methods in Physics Research Section A: Accelerators, Spectrometers, Detectors and Associated Equipment*, Vol. 954p. 161227, (2020).

34- Shelan T Mahmood, Kjell Erlandsson, Ian Cullum, and Brian Forbes Hutton, "Design of a novel slit-slat collimator system for SPECT imaging of the human brain." *Physics in Medicine & Biology*, Vol. 54 (No. 11), p. 3433, (2009).